Available online at www.sciencedirect.com
SCIENCE DIRECT®
Journal of Sound and Vibration 280 (2005) 595–610
JOURNAL OF SOUND AND VIBRATION
www.elsevier.com/locate/jsvi

Solving time-dependent engineering problems with multiquadrics

A.J.M. Ferreira*, P.A.L.S. Martins, C.M.C. Roque

Faculdade de Engenharia da Universidade do Porto, Departamento de Engenharia Mecânica e Gestão Industrial Rua Dr. Roberto Frias, 4200-465 Porto, Portugal

Received 24 February 2003; accepted 12 December 2003
Available online 3 September 2004

Abstract

This paper deals with the solution of time-dependent problems. The multiquadric radial basis function method is formulated, with a new approach for transient problems. One- and two-dimensional problems are considered. The forward difference and the Crank–Nicolson time-marching schemes for parabolic cases are considered. The central difference integration method of the Newmark family is considered for hyperbolic problems. The method proves its accuracy in four numerical examples.

1. Introduction

Time-dependent problems are of considerable relevance in engineering and science. This paper deals with the solution of time-dependent problems with radial basis functions. The multiquadric radial basis function method is formulated, with a new approach for transient problems. One- (1D) and two-dimensional (2D) problems are considered. The method proves its accuracy in some numerical 1D and 2D examples.

In this paper, a recent meshless approximation technique is used, based on radial basis functions (RBFs). This truly meshless technique is insensitive to spatial dimension, and considers

*Corresponding author. Tel.: +351-22-5081705; fax: +351-22-9537352.
E-mail address: ferreira@fe.up.pt (A.J.M. Ferreira).

0022-460X/$ - see front matter © 2004 Elsevier Ltd. All rights reserved.
doi:10.1016/j.jsv.2003.12.043

only a cloud of nodes (centers) for the spatial discretization of both the problem domain and the boundary.

Other meshless methods have also been proposed. They may be classified as smooth particle hydrodynamics [1–3], diffuse element method [4], element free Galerkin [5–7], reproducing kernel particle method [8–13] and HP clouds [14]. In recent years, Liu's group gave significant contributions, namely the local point interpolation method (LPIM) and the local radial point interpolation method (LR-PIM) [15,16], the radial point interpolation method (RPIM) [17] and the boundary radial point interpolation method (BRPIM) [18].

The radial basis function method was first used by Hardy [19,20] for the interpolation of geographical scattered data, and later used by Kansa [21,22] for the solution of partial differential equations (PDEs). Many other radial basis functions can be used as reviewed in the recent book of Liu [23], namely Powell [24], Coleman [25], Sharan et al. [26], Wendland [27], among others.

The use of RBFs for 2-D solids has been proposed by Liu et al. [28–30] and by Ferreira [31,32] for composite plates and beams. The method has also been applied to other engineering problems such as in Refs. [33–35].

This paper concentrates on the solutions of 1D and 2D engineering problems, such as heat conduction and beams in bending, using both the forward difference and Crank–Nicolson time-marching schemes with interpolation by the unsymmetrical multiquadric method.

2. The multiquadric method

The multiquadric method relies on the Euclidian distance between nodes and in some cases on a shape parameter (c), user-defined and object of various discussions. The influence of such parameters not only defines the RBF, but may also provide ill-conditioned problems with inadequate solutions.

The numerical solution of PDEs is traditionally dominated by finite element methods, finite volume methods or finite difference methods. All of these methods are based on local interpolation strategies and depend on a mesh for local approximation. In these methods, although the function is continuous across meshes, its partial derivatives are not [36–38].

A new approach for solving partial differential equations is based on RBFs. An RBF depends only on the distance to a center point $\mathbf{x}_j$ and is of the form $g(\|\mathbf{x}-\mathbf{x}_j\|)$. The RBF may also depend on a shape parameter c, in which case $g(\|\mathbf{x}-\mathbf{x}_j\|)$ is replaced by $g(\|\mathbf{x}-\mathbf{x}_j\|, c)$ [21,22,39–42].

Consider a set of nodes $x_1, x_2, \ldots, x_N \in \Omega \subset \mathbb{R}^n$. The radial basis functions centered at $\mathbf{x}_j$ are defined as

$$g_j(\mathbf{x}) \equiv g(\|\mathbf{x}-\mathbf{x}_j\|) \in \mathbb{R}^n, \quad j = 1, \ldots, N, \tag{1}$$

where $\|\mathbf{x}-\mathbf{x}_j\|$ is the Euclidian norm.

Some of the most common RBFs are [21,22,39–41]:

$$\text{Multiquadrics}: \quad g_j(\mathbf{x}) = (\|\mathbf{x}-\mathbf{x}_j\| + c^2)^{1/2}, \tag{2}$$

$$\text{Inverse Multiquadrics}: \quad g_j(\mathbf{x}) = (\|\mathbf{x}-\mathbf{x}_j\| + c^2)^{-1/2}, \tag{3}$$

$$\text{Gaussians}: \quad g_j(\mathbf{x}) = \mathrm{e}^{-c^2\|\mathbf{x}-\mathbf{x}_j\|^2}, \tag{4}$$

$$\text{Thin Plate Splines}: \quad g_j(\mathbf{x}) = \|\mathbf{x}-\mathbf{x}_j\|^2 \log\|\mathbf{x}-\mathbf{x}_j\|, \tag{5}$$

where c is a shape (user-defined) parameter. In this paper, only the multiquadric method is used.

RBFs are insensitive to spatial dimension, making the implementation of this method much easier than, e.g., finite elements [21,22].

Time-dependent problems have been treated with multiquadrics since their reappearance due to Kansa in 1990 [21,22]. Kansa applied his nonsymmetric multiquadric method to solve two parabolic and hyperbolic PDEs [22], the linear advection–diffusion equation and the dynamic 1D von Neumann blast wave. To solve the first problem, the author used a standard implicit approximation scheme; as for the second equation, a fourth-order Runge–Kutta scheme is used to perform the integration in time.

Another interesting approach to solve the 1D parabolic problem using RBFs came from Fasshauer [43], who made use of the Newton method and Nash iteration with an explicit time-stepping method to interpolate the classical Heat Equation.

Further incursions on the fluid dynamics domain have been made by authors like Hon and Wong [34]. They used the RBF meshless method to solve a multilayer computational model for simulating 3D tidal flows in coastal waters [44]. In this paper, the authors also prove the applicability of the RBF method in the solution of large-scale systems using a domain decomposition technique. They continued the exploration of hydrodynamic problems using RBF-based techniques, solving the Shallow water equations [34]. A different base of interpolating functions was used, the compactly supported RBFs or CSRBFs, which according to these authors allow application of RBF interpolation schemes in large-scale problems. Although simple, the forward differences scheme allowed authors to obtain an excellent match between experimental and observational data.

Multiquadrics are dependent only on space coordinates. This characteristic imposes the use of mixed algorithms to treat time-dependent problems. From Newton iteration to the forward differences scheme, it is possible to combine a wide variety of time-dependent solvers with the basic RBF spatial treatment, used for example in an homogeneous Poisson equation.

In this paper, it is proposed to use Kansa's unsymmetric collocation method [21,22]. For the purpose of completeness, a brief explanation of the method follows.

Consider a boundary-valued problem with a domain $\Omega \subset \mathbb{R}^n$ and a linear elliptic partial differential equation of the form

$$Lu(x) = s(x) \subset \mathbb{R}^n, \tag{6}$$

$$Bu(x)_{|\partial\Omega} = f(x) \in \mathbb{R}^n, \tag{7}$$

where $\partial\Omega$ represents the boundary of the problem. We use points along the boundary ($\mathbf{x}_j$, $j = 1,\ldots,N_B$) and in the interior ($\mathbf{x}_j$, $j = N_B+1,\ldots,N$).

Let the RBF interpolant to the solution $u(\mathbf{x})$ be

$$s(\mathbf{x}, c) = \sum_{j=1}^{N} \phi_j g(\|\mathbf{x} - \mathbf{x}_j\|, c). \tag{8}$$

Collocation with the boundary data at the boundary points and with PDE at the interior points leads to equations

$$s_B(\mathbf{x}, c) \equiv \sum_{j=1}^{N} \phi_j \, Bg(\|\mathbf{x} - \mathbf{x}_j\|, c) = \lambda(\mathbf{x}_i), \quad i = 1, \ldots, N_B, \tag{9}$$

$$s_L(\mathbf{x}, c) \equiv \sum_{j=1}^{N} \phi_j \, Lg(\|\mathbf{x} - \mathbf{x}_j\|, c) = \Phi(\mathbf{x}_i), \quad i = N_B + 1, \ldots, N, \tag{10}$$

where $\lambda(\mathbf{x}_i)$, $\Phi(\mathbf{x}_i)$ are the prescribed values at the boundary nodes and the function values at the interior nodes, respectively.

This corresponds to a system of equations with an unsymmetric coefficient matrix, structured in matrix form as

$$\begin{bmatrix} B\phi \\ L\phi \end{bmatrix} [\mathbf{a}] = \begin{bmatrix} \lambda \\ \mathbf{\Phi} \end{bmatrix}. \tag{11}$$

It has been shown that the unsymmetric coefficient matrix can become ill-conditioned or singular [40].

The use of globally supported RBFs for large problems can bring problems due to the full populated matrices. To solve this drawback, a localization scheme is advisable. Domain decomposition methods [39,45] and localization of the basis functions [39,46] claim to be able to deal with tens of thousands of nodes.

The present model does not issue such methods, as for problems dealt with in the paper the number of nodes to provide good quality solutions is usually small. For large applications involving analysis of plates and shells, such refined approaches are certainly needed.

3. Solving time-dependent problems

Consider the following general time-dependent problem:

$$\frac{\partial u}{\partial t} + Lu = f(x), \quad x \in \Omega, \tag{12}$$

where Ω is a domain in $\mathbb{R}^d$, $d = 1, 2, \ldots, n$ with boundary $\partial\Omega$ and L is some differential operator.

We approximate u by $\widetilde{u}$ and assume

$$\widetilde{u}(t, x) = \sum_{j=1}^{N} a_j(t) \phi(\|x - x_j\|, c), \tag{13}$$

where x_j are N distinct data points in Ω, and a_j's are unknown coefficients to be determined at each time step.

The derivative of the approximating solution on time is

$$\frac{\partial \widetilde{u}}{\partial t} = \sum_{j=1}^{N} \frac{\mathrm{d}a_j}{\mathrm{d}t}\, \phi(\|x - x_j\|, c). \tag{14}$$

Spatial derivatives are obtained as

$$\frac{\partial \widetilde{u}}{\partial x} = \sum_{j=1}^{N} a_j\, \frac{\partial \phi}{\partial x}\, \phi(\|x - x_j\|, c), \tag{15}$$

$$\frac{\partial^2 \widetilde{u}}{\partial x^2} = \sum_{j=1}^{N} a_j\, \frac{\partial^2 \phi}{\partial x^2}\, \phi(\|x - x_j\|, c) \cdots \tag{16}$$

Substituting Eqs. (13)–(16) into Eq. (12) and collocating at N points x_i, gives

$$\frac{\partial \widetilde{u}(x_i)}{\partial t} + L\widetilde{u}(x_i) = f(x_i), \tag{17}$$

which can be expressed as

$$\mathbf{\Phi}\dot{\mathbf{a}} + \mathbf{\Phi}_L \mathbf{a} = \mathbf{f}, \tag{18}$$

where $\mathbf{a}$ is the vector of unknown coefficients (a_j), $\mathbf{f}$ is the vector $f(x_i)$ and the matrices $\mathbf{\Phi}$ and $\mathbf{\Phi}_L$ are given by $\mathbf{\Phi} = \phi(\|x - x_j\|, c)$ and $\mathbf{\Phi}_L = L\phi(\|x - x_j\|, c)$, respectively.

Eq. (18) can be expressed as

$$\dot{\mathbf{a}} = -\mathbf{\Phi}^{-1}\mathbf{\Phi}_L \mathbf{a} + \mathbf{\Phi}^{-1}\mathbf{f}. \tag{19}$$

This is a typical system of first-order linear differential equations. With a time difference scheme applied to Eq. (19), the unknown coefficients $\mathbf{a}$ can be determined at each time step t if and only if the coefficient matrix $\mathbf{\Phi}$ is solvable.

To illustrate this problem more clearly, the first-order time difference scheme is applied to Eq. (18) obtaining

$$\mathbf{\Phi}\mathbf{a}^{n+1} = \mathbf{\Phi}\mathbf{a}^{n} - \Delta t \mathbf{\Phi}_L \mathbf{a} + \Delta t \mathbf{f}. \tag{20}$$

At each time step, n, the right-hand term of Eq. (19) is known, so Eq. (19) is similar to $\mathbf{\Phi}\mathbf{a} = \mathbf{f}$, the typical interpolation problem.

The following algorithm for time-dependent problems can now be formulated as

1. Initialize at time $t := 0$, approximate the initial condition using Eq. (13) and then compute the partial differential operator $L = L(u_0, u_x, u_{xx}, \ldots)$.
2. Solve Eq. (19) with some time-marching scheme to obtain coefficients $\mathbf{a}$ and then compute the solution $\mathbf{u}$ using Eq. (13) and the operator L at time $t := t$.
3. Correct the boundary values using boundary conditions.
4. Put $t := t + \Delta t$ and go to Step 2.

In the present paper, the Crank–Nicolson scheme was also used for parabolic problems.

In this case, the algorithm is established as follows. Consider a parabolic case. In the Crank–Nicolson formulation, the following two expressions hold for function and first derivative:

$$u^{t+\Delta t/2} = \tfrac{1}{2}(u^t + u^{t+\Delta t}), \tag{21}$$

$$\dot{u}^{t+\Delta t/2} = \frac{u^{t+\Delta t} - u^t}{\Delta t}. \tag{22}$$

When applying this scheme, the following equation is obtained:

$$u^{t+1} = u^t + \frac{\Delta t}{2}\left(\left(\frac{\mathrm{d}u}{\mathrm{d}t}\right)^{t+1} + \left(\frac{\mathrm{d}u}{\mathrm{d}t}\right)^{t}\right) \tag{23}$$

or

$$u^{t+1} - \frac{\Delta t}{2}\left(\frac{\mathrm{d}u}{\mathrm{d}t}\right)^{t+1} = u^t + \frac{\Delta t}{2}\left(\frac{\mathrm{d}u}{\mathrm{d}t}\right)^{t}. \tag{24}$$

The multiquadrics interpolation results in

$$\mathbf{\Phi a}^{n+1} - \frac{\Delta t}{2}\mathbf{\Phi}_L\mathbf{a}^{n+1} = \mathbf{\Phi a}^n + \frac{\Delta t}{2}\,\mathbf{\Phi}_L\mathbf{a}^n. \tag{25}$$

The remaining procedure follows the same scheme as in the forward difference approach.

The central difference integration method of the Newmark family was used for hyperbolic problems, such as beams in bending. The algorithm for this case follows a similar radial basis interpolation approach as in the parabolic formulations.

4. Examples and discussion

4.1. 1D heat-conduction problem

Consider a 1D heat-conduction problem, with equation

$$\frac{\partial u}{\partial t} - \frac{\partial^2 u}{\partial x^2} = 0, \quad 0 < x < 1$$

with boundary conditions

$$u(0,t) = 0, \quad \frac{\partial u}{\partial x}(1,t) = 0$$

and initial condition $u(x,0) = 1.0$. The problem is solved for time $0 \leqslant t \leqslant 1$, using $\Delta t = 0.05$. The grid used for this example is a regular grid as shown in Fig. 1.

As can be seen from Fig. 2 and Table 1, results obtained from the present methodology are in excellent agreement with exact results. Results are less adequate for $N \leqslant 5$.

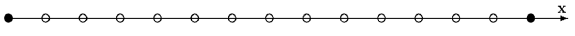

Fig. 1. Regular grid used for heat-conduction problem; ○ — boundary nodes; • — interior nodes.

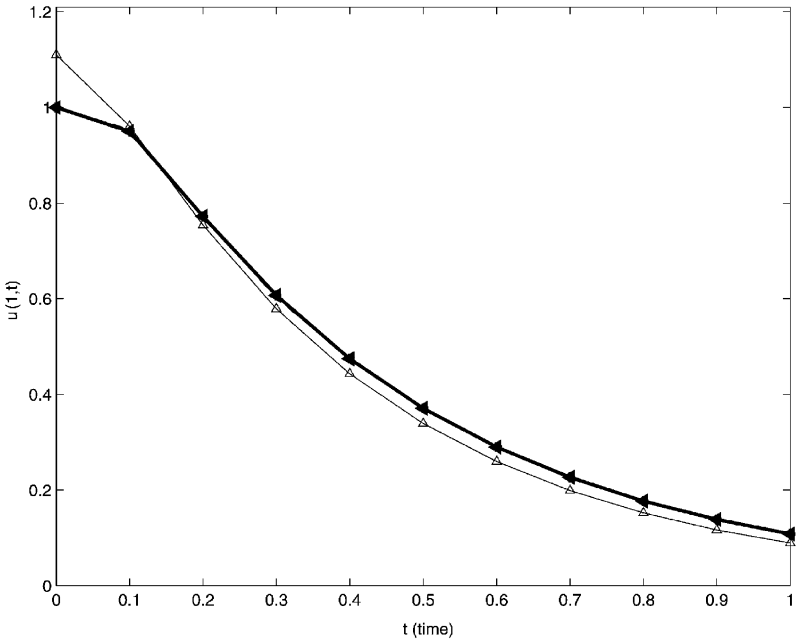

Fig. 2. 1D heat equation results; —△—, $N=5$; ——, $N=10$; ▲, $N=15$.

Table 1
1D heat-conduction problem—a comparison of the present model ($N = 5$, 10 and 15) with the exact solution and finite element solution of Reddy [47, p. 236]

Time t	Reddy [47]	Exact solution	$N = 5$	$N = 10$	$N = 15$
0.00	1.0000	1.0000	1.1103	1.0000	1.0000
0.10	0.9549	0.9493	0.9607	0.9520	0.9502
0.20	0.7731	0.7723	0.7541	0.7749	0.7726
0.30	0.6006	0.6068	0.5786	0.6097	0.6069
0.40	0.4741	0.4745	0.4430	0.4775	0.4746
0.50	0.3701	0.3708	0.3392	0.3738	0.3709
0.60	0.2890	0.2897	0.2596	0.2926	0.2898
0.70	0.2258	0.2264	0.1987	0.2290	0.2265
0.80	0.1764	0.1769	0.1522	0.1793	0.1769
0.90	0.1378	0.1382	0.1165	0.1403	0.1383
1.00	0.1076	0.1080	0.0892	0.1098	0.1081

4.2. Transverse motion of Bernoulli and Timoshenko beams

Consider the transverse motion of an isotropic beam, clamped at both ends, according to the Euler–Bernoulli beam theory, with equation

$$\frac{\partial^2 w}{\partial t^2} - \frac{\partial^4 w}{\partial x^4} = 0, \quad 0 < x < 1,$$

with boundary conditions

$$w(0,t)=0, \quad \frac{\partial w}{\partial x}(0,t)=0, \quad w(1,t)=0, \quad \frac{\partial w}{\partial x}(1,t)=0$$

and initial condition

$$w(x,0)=\sin \pi x-\pi x(1-x), \quad \frac{\partial w}{\partial t}(x,0)=0.$$

The problem is solved for time $0\leqslant t\leqslant 0.15$ using $\Delta t=0.005$ and the present solution compared with a finite element solution by Reddy [47], using four beam elements and a Galerkin solution. The grid for Bernoulli beams is illustrated in Fig. 3.

The present model presents results in excellent agreement with the exact solution and with the finite element results of Reddy [47]. The agreement improves, as expected, with the increase of grid points, as seen in Table 2 and Fig. 4. The modelling of the Euler–Bernoulli beam needs the consideration of the following boundary conditions, imposed upon the transverse deflection (w) and x-direction bending moment (M_x):

$$\text{(a) } w=0 \quad \text{in } x=0 \text{ and } x=L(\Gamma_1),$$

$$\text{(b) } M_x=0 \quad \text{in } \Gamma_2.$$

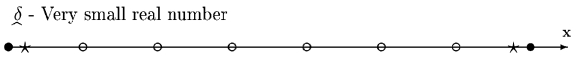

Fig. 3. Irregular grids for Euler–Bernoulli beams, Neumann conditions imposed; • — $w=0$ condition (Γ_1); ⋆ — $M_x=0$ condition (Γ_2); ○ — interior nodes.

Table 2
Transient Bernoulli beam—a comparison of the present model ($N=9$, 11 and 15) with the exact (Galerkin) solution and finite element solution of Reddy [47, p. 240]

Time t	Reddy [47]	Exact solution	$N=9$	$N=11$	$N=15$
0.00	0.2146	0.2146	0.2146	0.2146	0.2146
0.01	0.2098	0.2157	0.2106	0.2095	0.2089
0.02	0.1951	0.1988	0.2005	0.2001	0.1985
0.03	0.1698	0.1716	0.1655	0.1674	0.1691
0.04	0.1350	0.1356	0.1186	0.1252	0.1304
0.05	0.0935	0.0925	0.0654	0.0738	0.0818
0.06	0.0483	0.0447	0.0214	0.0306	0.0384
0.07	0.0018	−0.0055	−0.0292	−0.0189	−0.0107
0.08	−0.0455	−0.0553	−0.0830	−0.0693	−0.0586
0.09	−0.0923	−0.1023	−0.1397	−0.1245	−0.1111
0.10	−0.1336	−0.1441	−0.1760	−0.1644	−0.1520
0.11	−0.1682	−0.1783	−0.1986	−0.1917	−0.1834
0.12	−0.1932	−0.2034	−0.2091	−0.2048	−0.1996
0.13	−0.2087	−0.2179	−0.2202	−0.2172	−0.2136
0.14	−0.2148	−0.2211	−0.2144	−0.2171	−0.2164
0.15	−0.2111	−0.2129	−0.1904	−0.2022	−0.2094

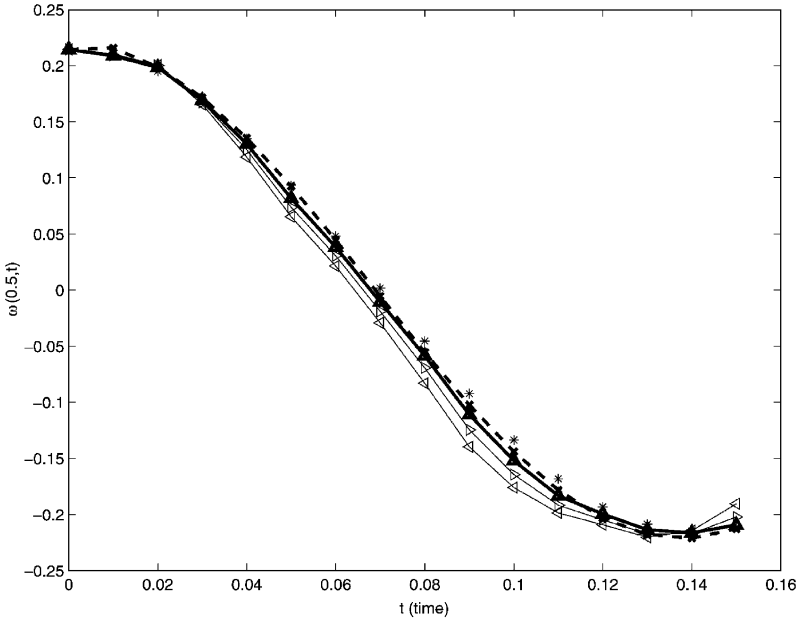

Fig. 4. Bernoulli beam results; *, Reddy [41]; —✖—, Exact; —◁—, $N=9$; —▷—, $N=11$; —▲—, $N=15$.

Due to the collocation strategy, it is necessary to impose the boundary condition defined in (b) in a near point: $M_x = 0$ in $x = 0 + \delta$; $x = L - \delta(\Gamma_2)$, where δ is a very small number. This type of boundary condition produces significant improvement over boundary conditions imposed on regular grids (Fig. 3).

Another method for dealing with superposition of boundary conditions was proposed by Wu and his colleagues [48–54].

The evolution of the transverse displacement with time for larger times is illustrated in Fig. 5. It can be seen that a very regular pattern is obtained without divergence of the solution. It is now considered the same beam problem, but with a Timoshenko formulation with $h = 0.01$ and 0.1.

The governing equations of the Timoshenko beam with cross section A are given by

$$\rho A \frac{\partial^2 w}{\partial t^2} - \frac{\partial}{\partial x}\left[GAk\left(\frac{\partial w}{\partial x} + \phi\right)\right] = 0, \tag{26}$$

$$\rho I \frac{\partial^2 \phi}{\partial t^2} - \frac{\partial}{\partial x}\left[EI\frac{\partial \phi}{\partial x}\right] + GAk\left(\frac{\partial w}{\partial x} + \phi\right) = 0, \tag{27}$$

where G is the shear modulus, K is the shear correction coefficient, ρ is the material density and I the inertia moment.

In order to present a similar simulation as in the case of the Euler–Bernoulli beam, consider $\mathrm{EI} = 1.0$, $\rho A = 1.0$.

In Fig. 6 and Table 3, results are presented and compared with a Galerkin formulation and finite element results of Reddy [47]. Again, $\Delta t = 0.005$ is used as in Reddy's book, with central

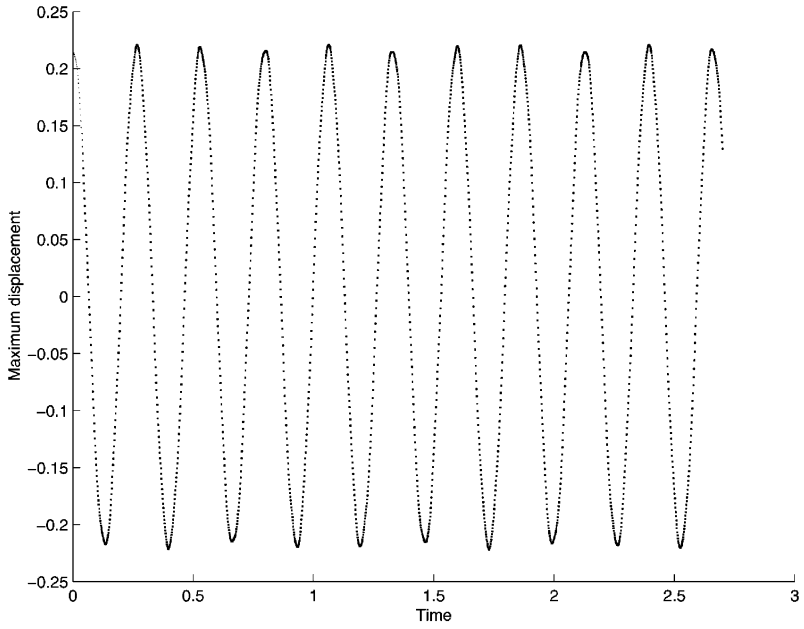

Fig. 5. Evolution of displacement with time.

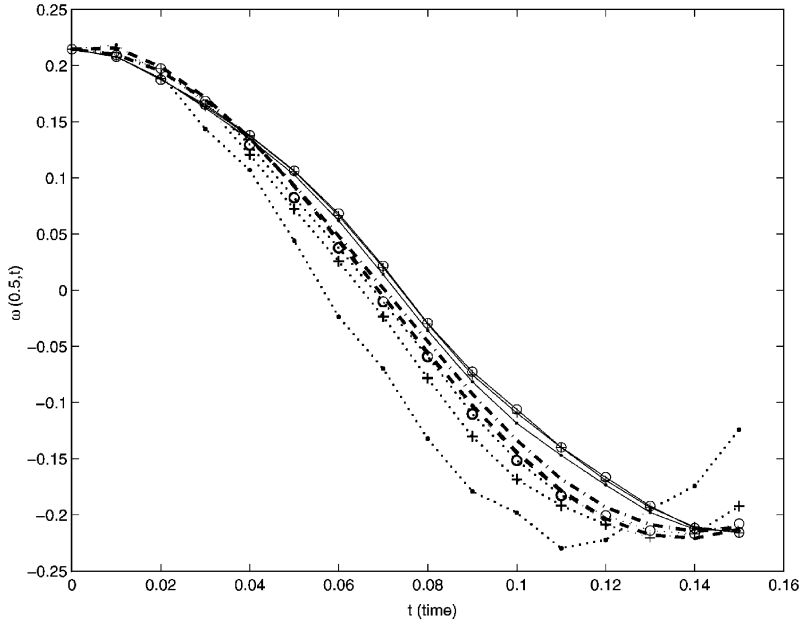

Fig. 6. Timoshenko beam results. ▪ ▪ ▪, Reddy [41]; ▬ ▬, Galerkin; · · ● · ·, $h=0.01$, $N=7$; · + ·, $h=0.01$, $N=9$; · ○ ·, $h=0.01$, $N=11$; —●—, $h=0.1$, $N=7$; —┼—, $h=0.1$, $N=9$; -○-, $h=0.1$, $N=11$.

difference (Newmark) scheme. Results with $h=0.01$ or 0.1 agree quite well with both formulations. The grid used in this case is similar to the one illustrated in Fig. 1.

In general, the methodology presents quite good results.

Table 3
Transient Timoshenko beam—a comparison of the present model ($N = 7$, 9 and 11) with the exact solution and finite element solution of Reddy [47, p. 240]

Time t	Reddy [47]	Galerkin	$h = 0.01$			$h = 0.1$		
			$N = 7$	$N = 9$	$N = 11$	$N = 7$	$N = 9$	$N = 11$
0.00	0.2146	0.2146	0.2146	0.2146	0.2146	0.2146	0.2146	0.2146
0.01	0.2098	0.2157	0.2185	0.2113	0.2096	0.2080	0.2077	0.2079
0.02	0.1951	0.1988	0.1922	0.1972	0.1974	0.1887	0.1883	0.1875
0.03	0.1698	0.1716	0.1436	0.1659	0.1684	0.1622	0.1636	0.1652
0.04	0.1350	0.1356	0.1070	0.1207	0.1294	0.1347	0.1375	0.1379
0.05	0.0935	0.0925	0.0440	0.0723	0.0824	0.1028	0.1059	0.1064
0.06	0.0483	0.0447	0.0236	0.0258	0.0379	0.0620	0.0663	0.0682
0.07	0.0018	−0.0055	−0.0699	−0.0235	−0.0102	0.0140	0.0202	0.0217
0.08	−0.0455	−0.0553	−0.1323	−0.0784	−0.0590	−0.0358	−0.0301	−0.0293
0.09	−0.0923	−0.1023	−0.1792	−0.1304	−0.1103	−0.0815	−0.0754	−0.0726
0.10	−0.1336	−0.1441	−0.1981	−0.1684	−0.1515	−0.1185	−0.1093	−0.1061
0.11	−0.1682	−0.1783	−0.2297	−0.1919	−0.1826	−0.1472	−0.1402	−0.1399
0.12	−0.1932	−0.2034	−0.2224	−0.2086	−0.2006	−0.1735	−0.1693	−0.1666
0.13	−0.2087	−0.2179	−0.1952	−0.2202	−0.2141	−0.1979	−0.1934	−0.1922
0.14	−0.2148	−0.2211	−0.1744	−0.2169	−0.2169	−0.2129	−0.2108	−0.2118
0.15	−0.2111	−0.2129	−0.1242	−0.1923	−0.2079	−0.2142	−0.2161	−0.2157

4.3. 2D Poisson problem

Consider the 2D Poisson transient problem, with equation

$$\frac{\partial T}{\partial t} - \nabla^2 T = 1, \quad \text{in } \Omega = \{(x,y): 0 < (x,y) < 1\},$$

with boundary conditions

$$T = 0 \quad \text{on } \Gamma_1 = \{\text{Lines } x = 1 \text{ and } y = 1\}, \quad t \geqslant 0,$$

$$\frac{\partial T}{\partial n} = 0 \quad \text{on } \Gamma_2 = \{\text{Lines } x = 0 \text{ and } y = 0\}, \quad t \geqslant 0$$

and initial condition

$$T = 0, \quad \text{in } \Omega.$$

The square grid used in this example is shown in Fig. 7. The problem is solved for time $0 \leqslant t \leqslant 1.0$. In Table 4 and Fig. 8, the present method is compared with the finite element results of Reddy [55] and shows high accuracy.

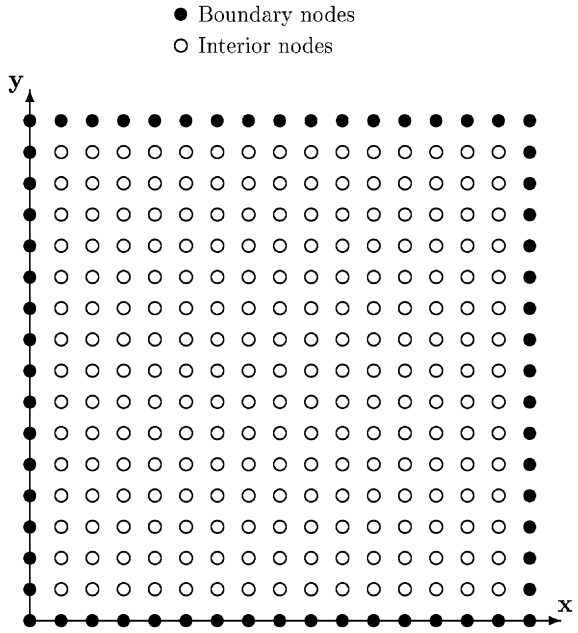

Fig. 7. Grid for 2D problems.

Table 4
Transient 2D Poisson—a comparison of the present model ($N = 5, 9$ and 17) with the exact solution and finite element solution of Reddy [55, p. 240]

Time t	Formulation	Temperature along the $y = 0$ line ($T(x, 0, t) \times 10$)			
		$x = 0.0$	$x = 0.25$	$x = 0.50$	$x = 0.75$
0.1	Reddy [55] (R2)	0.9945	0.9853	0.9264	0.6360
	5×5 grid	1.0580	1.0182	0.9195	0.6451
	9×9 grid	0.9872	0.9673	0.8822	0.6258
	17×17 grid	0.9841	0.9718	0.9020	0.6323
0.2	Reddy [55] (R2)	1.8115	1.7329	1.4997	0.9612
	5×5 grid	1.8272	1.7395	1.4881	0.9607
	9×9 grid	1.7376	1.6699	1.4365	0.9347
	17×17 grid	1.7257	1.6597	1.4275	0.9274
0.3	Reddy [55] (R2)	2.2479	2.1432	1.8018	1.1319
	5×5 grid	2.3058	2.1845	1.8309	1.1147
	9×9 grid	2.2117	2.1090	1.7742	1.1183
	17×17 grid	2.1998	2.0982	1.7644	1.1102
1.0	Reddy [55] (R2)	2.9621	2.8037	2.3065	1.4053
	5×5 grid	3.0131	2.8413	2.3352	1.4187
	9×9 grid	2.9308	2.7740	2.2836	1.3941
	17×17 grid	2.9237	2.7672	2.2767	1.3878

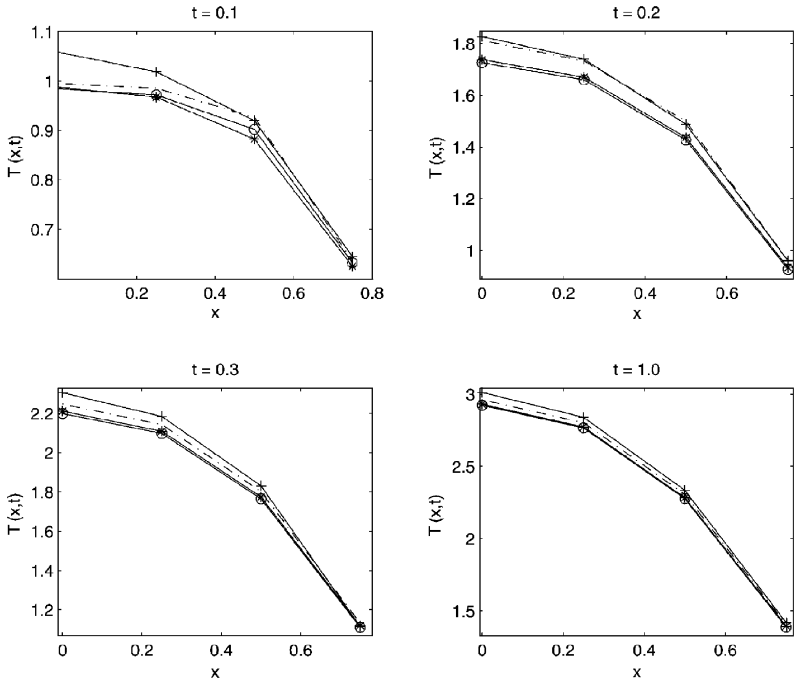

Fig. 8. 2D Poisson results.

5. Conclusions

In this paper, the multiquadric radial basis function method was applied to the analysis of some time-dependent problems. A one- and two-dimensional conduction and a beam in bending were analyzed. Euler–Bernoulli and Timoshenko formulations were used for the transient analysis of isotropic beams. Results were compared with existing solutions showing excellent performance.

Results showed that the use of unsymmetric colocation strategy gives very good agreement with available theories or previous results for all cases.

This method, based on radial basis functions has very large potential for the solution of structural problems, as a real meshless method, insensible to spatial dimension.

Acknowledgements

The support of Fundação para a Ciência e a Tecnologia, under Financiamento Plurianual (Unidade Mecânica Experimental e Novos Materiais) is gratefully acknowledged.

References

[1] P.W. Randles, L.D. Libersky, Smoothed particle hydrodynamics: some recent improvements and applications, *Computer Methods in Applied Mechanics and Engineering* 139 (1996) 375–408.

[2] T. Belytschko, Y. Krongauz, D. Organ, M. Fleming, P. Krysl, Meshless methods: an overview and recent developments, *Computer Methods in Applied Mechanics and Engineering* 139 (1996) 3–47.
[3] J. Bonet, S. Kulasegaram, Correction and stabilization of smooth particle hydrodynamics methods with applications in metal forming simulations, *International Journal of Numerical Methods in Engineering* 47 (2000) 1189–1214.
[4] B. Nayroles, G. Touzot, P. Villon, Generalizing the finite element method: diffuse approximation and diffuse elements, *Computational Mechanics* 10 (1992) 307–318.
[5] T. Belytschko, Y.Y. Lu, L. Gu, Element free Galerkin methods, *International Journal of Numerical Methods in Engineering* 37 (1994) 229–256.
[6] J.P. Ponthot, T. Belytschko, Arbitrary Lagrangian–Eulerian formulation for element-free Galerkin method, *Computer Methods in Applied Mechanics and Engineering* 152 (1998) 19–46.
[7] B. William, S. Saigal, A three-dimensional element-free Galerkin elastic and elastoplastic formulation, *International Journal of Numerical Methods in Engineering* 46 (1999) 671–693.
[8] W.K. Liu, S. Jun, Y.F. Zhang, Reproducing kernel particle methods, *International Journal of Numerical Methods in Fluids* 20 (1995) 1081–1106.
[9] W.K. Liu, S. Jun, S. Li, J. Adee, T. Belytschko, Reproducing kernel particle methods for structural dynamics, *International Journal of Numerical Methods in Engineering* 38 (1995) 1655–1679.
[10] W.K. Liu, S. Jun, Multiple-scale reproducing kernel particle methods for large deformation problems, *International Journal of Numerical Methods in Engineering* 41 (1998) 1339–1362.
[11] K.M. Liew, T.Y. Ng, Y.C. Wu, Meshfree method for large deformation analysis—a reproducing kernel particle approach, *Engineering Structures* 24 (2002) 543–551.
[12] K.M. Liew, T.Y. Ng, X. Zhao, J.N. Reddy, Harmonic reproducing kernel particle method for free vibration of rotating cylindrical shells, *Computer Methods in Applied Mechanics and Engineering* 191 (2002) 4141–4157.
[13] K.M. Liew, H.Y. Wu, T.Y. Ng, Meshless method for modeling of human proximal femur: treatment of nonconvex boundaries and stress analysis, *Computational Mechanics* 28 (2002) 390–400.
[14] C.A. Duarte, J.T. Oden, An HP adaptive method using clouds, *Computer Methods in Applied Mechanics and Engineering* 139 (1996) 237–262.
[15] G.R. Liu, Y.T. Gu, Comparisons of two meshfree local point interpolation methods for structural analyses, *Computational Mechanics* 29 (2) (2002) 107–121.
[16] G.R. Liu, K.Y. Dai, Y.T. Gu, A radial point interpolation method for simulation of two-dimensional piezoelectric structures, *Smart Materials and Structures* 12 (2003) 171–180.
[17] G.R. Liu, J.G. Wang, Y.T. Gu, Point interpolation method based on local residual formulation using radial basis functions, *Structural Engineering and Mechanics* 14 (6) (2002) 713–732.
[18] Y.T. Gu, G.R. Liu, A boundary radial point interpolation method (BRPIM)for 2-D structural analyses, *Computational and Applied Mathematics* 145 (2002) 223–235.
[19] R.L. Hardy, Multiquadric equations of topography and other irregular surfaces, *Geophysical Research* 176 (1971) 1905–1915.
[20] R.L. Hardy, Theory and applications of the multiquadric-biharmonic method: 20 years of discovery, *Computers & Mathematics with Applications* 19 (8/9) (1990) 163–208.
[21] E.J. Kansa, Multiquadrics—a scattered data approximation scheme with applications to computational fluid dynamics—part I: surface approximations and partial derivative estimates, *Computers & Mathematics with Applications* 19 (8/9) (1990) 127–145.
[22] E.J. Kansa, Multiquadrics—a scattered data approximation scheme with applications to computational fluid dynamics—part II: solutions to parabolic, hyperbolic and elliptic partial differential equations, *Computers & Mathematics with Applications* 19 (8/9) (1990) 147–161.
[23] G.R. Liu, *Mesh Free Methods*, CRC Press, Boca Raton, USA, 2003.
[24] M.J.D. Powell, The theory of radial basis function approximation in 1990, in: F.W. Light (Ed.), *Advances in Numerical Analysis*, Oxford University Press, Oxford, 1992, pp. 203–240.
[25] C.J. Coleman, On the use of radial basis functions in the solution of elliptic boundary value problems, *Computational Mechanics* 17 (1996) 418–422.

[26] M. Sharan, E.J. Kansa, S. Gupta, Application of the multiquadric method for numerical solution of elliptic partial differential equations, *Applied Mathematics and Computation* 84 (1997) 275–302.
[27] H. Wendland, Error estimates for interpolation by compactly supported radial basis functions of minimal degree, *Journal of Approximation Theory* 93 (1998) 258–296.
[28] G.R. Liu, Y.T. Gu, A local radial point interpolation method (LRPIM) for free vibration analyses of 2-D solids, *Journal of Sound and Vibration* 246 (1) (2001) 29–46.
[29] G.R. Liu, J.G. Wang, A point interpolation meshless method based on radial basis functions, *International Journal of Numerical Methods in Engineering* 54 (2002) 1623–1648.
[30] J.G. Wang, G.R. Liu, On the optimal shape parameters of radial basis functions used for 2-D meshless methods, *Computational Methods in Applied Mechanics and Engineering* 191 (2002) 2611–2630.
[31] A.J.M. Ferreira, A formulation of the multiquadric radial basis function method for the analysis of laminated composite plates, *Composite Structures* 59 (2003) 385–392.
[32] A.J.M. Ferreira, Thick composite beam analysis using a global meshless approximation based on radial basis functions, *Mechanics of Advanced Materials and Structures* 10 (2003) 271–284.
[33] Y.C. Hon, M.W. Lu, W.M. Xue, Y.M. Zhu, Multiquadric method for the numerical solution of byphasic mixture model, *Applied Mathematics and Computation* 88 (1997) 153–175.
[34] Y.C. Hon, K.F. Cheung, X.Z. Mao, E.J. Kansa, A multiquadric solution for the shallow water equation, *Journal of Hydraulic Engineering* 125 (5) (1999) 524–533.
[35] J.G. Wang, G.R. Liu, P. Lin, Numerical analysis of biot's consolidation process by radial point interpolation method, *International Journal of Solids and Structures* 39 (6) (2002) 1557–1573.
[36] O.C. Zienkiewicz, *The Finite Element Method*, McGraw-Hill, New York, 1991.
[37] T.J.R. Hughes, *The Finite Element Method—Linear Static and Dynamic Finite Element Analysis*, Dover Publications, New York, 2000.
[38] K.J. Bathe, *Finite Element Procedures in Engineering Analysis*, Prentice-Hall, Englewood Cliffs, NJ, 1982.
[39] E.J. Kansa, Y.C. Hon, Circunvecting the ill-conditioning problem with multiquadric radial basis functions, *Computers & Mathematics with Applications* 39 (7–8) (2000) 123–137.
[40] G.E. Fasshauer, Solving partial differential equations by collocation with radial basis functions, Surface fitting and multiresolution methods *Proceedings of the Third International Conference on Curves and Surfaces*, Vol.2, 1997, pp. 131–138.
[41] Y.C. Hon, X.Z. Mao, On unsymmetric collocation by radial basis functions, *Applied Mathematics and Computations* 119 (2–3) (2001) 177–186.
[42] R.K. Beatson, Fast fitting of radial basis functions: methods based on preconditioned gmres iteration, *Advances in Computational Mathematics* 11 (1999) 253–270.
[43] G.E. Fasshauer, Newton iteration with multiquadrics for the solution of nonlinear PDEs, *Computers & Mathematics with Applications* 43 (2002) 423–438.
[44] S.M. Wong, Y.C. Hon, T.S. Li, A meshless multilayer model for a coastal system by radial basis functions, *Computers & Mathematics with Applications* 43 (2002) 585–605.
[45] M.R. Dubal, S.R. Oliveira, R.A. Matzner, Domain decomposition and local refinement for multiquadric approximations—part I: second-order equations in one-dimension, *Journal of Applied Science and Computers* 1 (1994) 146–171.
[46] R.K. Beatson, W.A. Light, Fast evaluation of radial basis functions: methods for 2-dimensional polyharmonic splines, *IMA Journal of Numerical Analysis* 17 (1997) 343–372.
[47] J.N. Reddy, *An Introduction to the Finite Element Method*, McGraw-Hill International Editions, New York, 1993.
[48] G.R. Liu, T.Y. Wu, Multipoint boundary value problems by differential quadrature method, *Mathematical and Computer Modelling* 35 (2002) 215–227.
[49] T.Y. Wu, G.R. Liu, The generalized differential quadrature rule for initial-value differential equations, *Journal of Sound and Vibration* 233 (2) (2000) 213–295.
[50] T.Y. Wu, G.R. Liu, Axisymmetric bending solution of shells of revolution by the generalized differential quadrature rule, *International Journal of Pressure Vessels and Piping* 77 (4) (2000) 149–157.
[51] G.R. Liu, T.Y. Wu, Numerical solution for differential equations of a duffing-type non-linearity using the generalized differential quadrature rule, *Journal of Sound and Vibration* 237 (5) (2000) 805–817.

[52] T.Y. Wu, G.R. Liu, The generalized differential quadrature rule for fourth-order differential equations, *International Journal of Numerical Methods in Engineering* 50 (2001) 1927–1929.
[53] T.Y. Wu, G.R. Liu, Application of the generalized differential quadrature rule to sixth-order differential equations, *Communications in Numerical Methods in Engineering* 16 (11) (2000) 777–784.
[54] G.R. Liu, T.Y. Wu, Differential quadrature solutions of eight-order boundary-value differential equations, *Computational and Applied Mathematics* 145 (2002) 223–235.
[55] J.N. Reddy, *Applied Functional Analysis and Variational Methods in Engineering*, McGraw-Hill International Editions, New York, 1986.